Arrhythmia Detection with Antidictionary Coding and Its Application on Mobile Platforms

Gilson Frias[1(✉)], Hiroyoshi Morita[1], and Takahiro Ota[2]

[1] The University of Electro-Communications, Chofu, Tokyo 182-8585, Japan
gilson.frias@mail.uec.jp, morita@uec.ac.jp
[2] Nagano Prefectural Institute of Technology, Ueda, Nagano 386-1211, Japan
ota@cse.pit-nagano.ac.jp
http://www.appnet.is.uec.ac.jp/

Abstract. In response to the demand of memory efficient algorithms for electrocardiogram (ECG) signal processing and anomaly detection on wearable and mobile devices, an implementation of the antidictionary coding algorithm for memory constrained devices is presented. Pre-trained *finite-state* probabilistic models built from quantized ECG sequences were constructed in an offline fashion and their performance was evaluated on a set of test signals. The low complexity requirements of the models is confirmed with a port of a pre-trained model of the algorithm into a mobile device without incurring on excessive use of computational resources.

Keywords: ECG · Arrhythmia · Antidictionary · Werable · Mobile

1 Introduction

The Internet of things (IoT) revolution has driven the use of wearable devices for fitness tracking and health monitoring, empowering patients with the capability of doing self assessments about their health condition. The use of such technologies is expected to increment in the foreseeable future [1]. In that sense, the ambulatory monitoring of electrocardiogram (ECG) signals has proven to be of great importance for the early detection and treatment of a broad range of cardiac diseases. The small form factor and low power consumption characteristics of modern ECG monitors assure the necessity of efficient algorithms for the processing of the biosignals. Moreover, efficient lossless compression schemes are required in order to reduce the amounts of disk space for storage and bandwidth for wireless transmission.

The algorithm for Data Compression with Antidictionaries (DCA), first introduced by *Crochemore et al.* [2], makes use of the set of patterns that never appear

This work is supported by JSPS KAKENHI Grant Number JP17K00400.

L. Mucchi et al. (Eds.): BODYNETS 2019, LNICST 297, pp. 50–67, 2019.
https://doi.org/10.1007/978-3-030-34833-5_5

on the source data set to effectively predict redundant symbols. The feasibility of the DCA for the compression of ECG signals has been previously studied, and it was also shown that the DCA method can be used for the detection of irregular heart beat patterns [3]. The algorithm constructs *finite-state* probabilistic models with the forbidden patterns obtained from the antidictionaries. The presence of expected patterns within the signals causes the algorithm to output a low and steady Compression Ratio, while the appearance of forbidden patterns such as those that occur on arrhythmias causes an increase on the Compression Ratio, thus enabling the DCA algorithm to be suitable for detection tasks.

It has been also shown that by translating the domain of the ECG distribution into a finite set of small integers it is possible to implement the detection algorithm with the use of less memory resources while maintaining an acceptable performance. This was done by the implementation of differentiation and a quantization stages on the signal processing chain that in effect redefines the signal in a restricted alphabet set [4].

In this paper, we present the results of porting the antidictionary coding algorithm into a mobile platform. Pre-trained models for the detection of Premature Ventricular Contractions (PVC) have been implemented on the IOS operating system, requiring relative small amounts of computational resources to process real time streams of ECG data transmitted through the Bluetooth Low Energy (LE) communication standard. Additionally, a new quantization method is introduced with the use of percentile statistical measurements from the ECG distribution.

Contents are presented in the following order: In Sect. 2 a brief overview on the characteristics of the ECG signal and the PVC arrhythmia will be presented. In Sect. 3 the theory behind Antidictionary Coding will be discussed. In Sect. 4, a description of the offline processing of the ECG is given, detailing the process involve in the construction of the probabilistic models and the selection criteria followed for picking the trained models used for a subsequent stage of online experimentation. Finally, in Sect. 5 the results of porting the offline-trained model into an IOS application for online processing of the ECG samples are shown.

2 The ECG Signal and Premature Ventricular Contractions

The Electrocardiogram (ECG) is a signal that represents the electrical activity of the heart. Usually measured directly on the body's surface, the ECG waveform is mainly composed of five characteristic components denoted by the letters P, Q, R, S and T. Each component marks the location of a specific peak or valley on the ECG signal that corresponds to a change in electrical activity in the heart and the consequent movement of the cardiac muscle. Sometimes an U component is also present following the T peak. The left part of Fig. 1 displays an overview of a typical ECG waveform. The P-peak on the waveform is generated with the activation of the upper chambers of the heart, the left and right atria, while the

QRS complex and the T-peak are generated with the activation process of the two lower chambers, the left and right ventricles [5].

The R-R interval is also pointed on the left side of Fig. 1, it is a measure of the time elapsed between consecutive heartbeats and is an important metric usually used for the calculation of the heart rate.

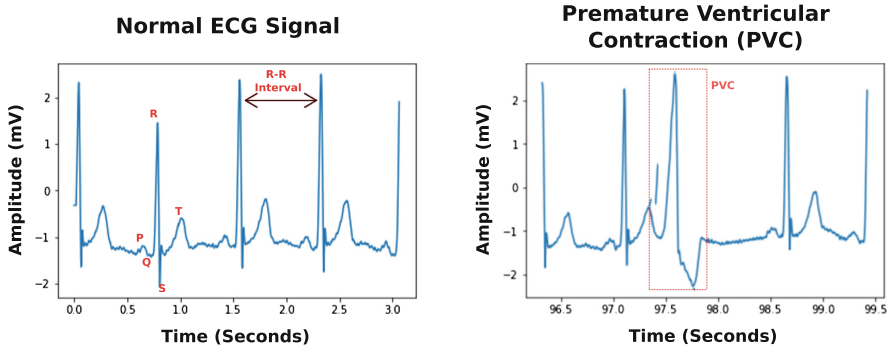

Fig. 1. Two ECG waveforms showing 4 heartbeats each. The second heartbeat on the left figure displays the location of main peaks and valleys that characterize the signal. The right figure shows an ECG waveform containing the occurrence of a PVC on the third heartbeat.

Premature Ventricular Contractions (PVC) are abnormal contractions that occur earlier than expected within the normal hearth cycle. The PVCs are generated on the ventricles, unlike the electrical impulses that drive the normal heart cycle, which are generated on the sinoatrial node [6]. The occurrence of PVCs can be an important indicator of the presence of an underlaying hearth disease, and they can be recognized on the ECG as abnormal and wide QRS complexes [7]. The right part of Fig. 1 shows an ECG waveform that contains one PVC. The occurrence of the premature heart beat disrupts the normal R-R interval and thus causing variability in the heart rate.

3 Finite State Machines (FSM) Probability Models with Antidictionaries

Let Σ_m be a finite set of integers $\{0, 1, \ldots, m-1\}$, called m-ary alphabet. For a string $\boldsymbol{x}^n = x_1 x_2 \ldots x_n$ of length n, we consider the set $\mathcal{D}(\boldsymbol{x}^n)$ called the dictionary of $\boldsymbol{x}^n$, as the set that contains all substrings of $\boldsymbol{x}^n$ including the null string $\boldsymbol{\lambda}$ of length zero. The antidictionary $\mathcal{A}(\boldsymbol{x}^n)$ of $\boldsymbol{x}^n$ is defined as the set of *minimal* strings that never appear in $\boldsymbol{x}^n$. An element $\boldsymbol{v} = v_1 v_2 \ldots v_k$ in $A(\boldsymbol{x}^n)$ is called Minimal Forbidden Word (MFW) which must satisfy the following three conditions:

1. $\boldsymbol{v} \notin \mathcal{D}(\boldsymbol{x}^n)$
2. A one-symbol shorter prefix of $\boldsymbol{v}$, defined as $p(\boldsymbol{v}) = v_1 v_2 ... v_{k-1}$, must be contained in $\mathcal{D}(\boldsymbol{x}^n)$.
3. A one-symbol shorter suffix of $\boldsymbol{v}$, defined as $s(\boldsymbol{v}) = v_2 v_3 ... v_k$, must be also contained in $\mathcal{D}(\boldsymbol{x}^n)$.

Data compression is achieved by the Data Compression using Antidictionary (DCA) algorithm [8]. From $\mathcal{A}(\boldsymbol{x}^n)$, a proper set of MFWs is selected for the construction of a finite state machine, hereafter referred as FSM. The FSM can be utilized to build a probabilistic model that normally accepts substrings of $\boldsymbol{x}^n$, but in the presence of an MFW it will lock itself in a terminal state. A simple example is introduced next to illustrate the concepts just established. Consider a string $\boldsymbol{w} = 2210010$ over $\Sigma_3 = \{0, 1, 2\}$. As discussed previously, the antidictionary $\mathcal{A}(\boldsymbol{w})$ of $\boldsymbol{w}$ is given by the set of all MFWs of $\boldsymbol{w}$, thus $\mathcal{A}(\boldsymbol{w}) = \{02, 000, 11, 12, 101, 20, 222, 0100\}$. By taking a subset of $\mathcal{A}(\boldsymbol{w})$, say $\mathcal{A}_s(\boldsymbol{w}) = \{02, 11, 20\}$, we construct a FSM probabilistic model, as shown in Fig. 2.

The FSM consists of seven states or nodes, with four states S_1, S_2, S_3 and S_4 being the internal states and the remaining three states R_1, R_2 and R_3 are the external states. Each internal state points to another state (or to itself) through an edge, in Fig. 2 an edge is defined by an arrow and the accompanying symbol that causes the transition to a new state.

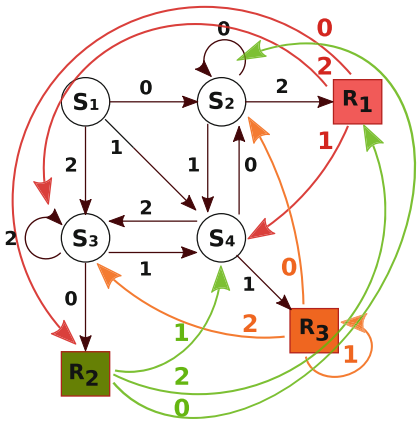

Fig. 2. An FSM model for MFWs 02, 11 and 20. Coloured edges denote the corresponding transitions after a forbidden state is reached. (Color figure online)

Now assume that the *ith* symbol of $\boldsymbol{x}^n (1 \leq i \leq n)$ is being processed by the FSM, and we define the next state reached sequentially by x_i as s_i, where $1 \leq i < n$ and s_0 denotes the initial state of the FSM. Moreover, we assume that the state sequence $s^m = s_0 s_1 \ldots s_m$ is uniquely determined by the input

string $\boldsymbol{x}^m = x_1 x_2 \ldots x_m (1 \leq m \leq n)$. The probability of transitioning to a state specified by the next symbol on the sequence, $P(x_{i+1}|s_i)$, is given by

$$P(x_{i+1}|s_i) = \frac{N(x_{i+1}|s_i)}{\sum_{c \in \Sigma} N(c|s_i)}, \quad 0 \leq i < n \tag{1}$$

where $N(c|s_i)$ denotes the number of times that a transition has happened from state s_i with symbol c.

The algorithm's output for a given symbol that is being encoded depends on whether the next transition leads to an internal state or to an external state. For a given integer sequence $1 \leq I_1 < I_2 < \cdots < I_{t+1} = n$, if the I_jth state $(1 \leq j \leq t)$ to be reached corresponds to an external state and the final state I_{t+1} does not necessary so, then it can be concluded that an MFW is present as a substring of the input sequence and the algorithm outputs the corresponding interval I_j of occurrence of the transition to the external state.

In the case of a transition to an external state s_i through symbol x_i, the algorithm would point next to the node that covers the sequence $v = x_{i-s} \ldots x_{i+1}$, where v coincides with the *Longest Common Prefix* with one MFW in $\mathcal{A}(\boldsymbol{w})$ and $(0 \leq s \leq i-1)$.

In the case that the transition leads to an internal state, the algorithm's output depends on the total number of available edges, denoted by n_E, that lead to terminal states from the current node. If $n_E = 1$, then the next symbol can be predicted and the algorithm does not output anything. However, if $n_E > 1$, then the algorithm outputs the transition probability $P(x_{i+1}|s_i)$ associated with the next symbol x_{i+1} [3].

4 Description of the Detection System

Figure 3 shows the structure of the proposed detection system. The details concerning each stage in the processing pipeline will be discussed next.

4.1 Signal Differentiation

The shape of the probability distribution constructed from the ECG signals can be affected by the presence of noise and unwanted artifacts in the signals [9]. The presence of arrhythmia components within the signal can also cause asymmetry and flattening on the distribution [10]. The left part of Fig. 4 shows a histogram built from an ECG record consisting of 650,000 samples (with 11 bit resolution). The distribution clearly displays the asymmetry and flattening characteristics discussed earlier.

The detection algorithm proposed in this study relies in a quantization process aiming to convey the information contained in the ECG probability distribution into a new distribution defined over a smaller alphabet set. The irregularities in the shape of the ECG distribution can lead to uneven distribution of the samples in the new probability distribution created from the quantized signals.

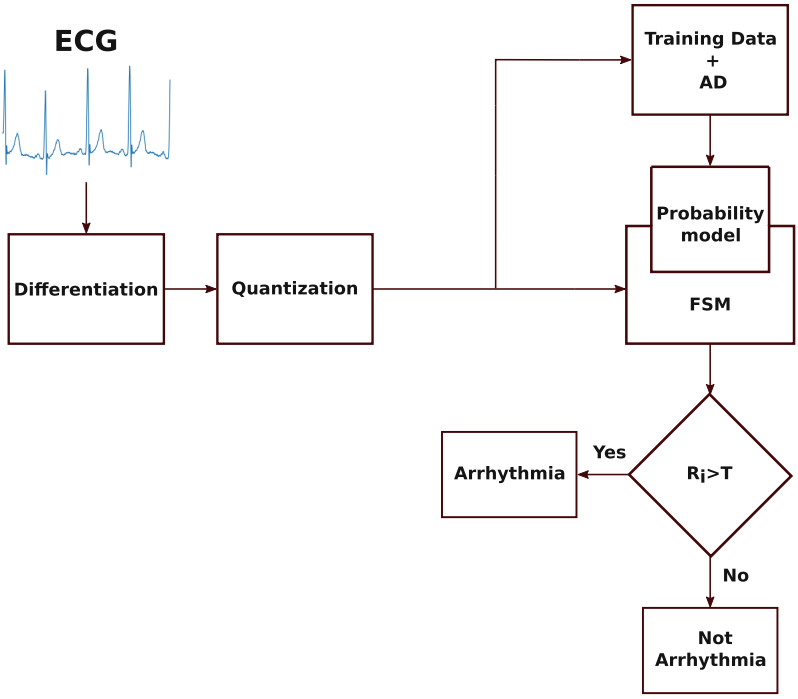

Fig. 3. Schematic diagram of the detection system.

To address this inconvenience, we introduce a differentiation step prior to the quantization process. In this context, we use the term *differentiation* to refer to the operation of subtraction of consecutive samples in the original signals.

For a sampled signal sequence denoted by $\boldsymbol{z}^n = z_1 z_2 \dots z_n$ where $z_i \in \Sigma_{2048}, 1 \leq i \leq n$, the differentiation process that yields the output sequence $\boldsymbol{y}^n = y_1 y_2 \dots y_n$ is stated as follows:

$$y_i = \begin{cases} z_i & i = 1 \\ z_i - z_{i-1} & 1 < i \leq n \end{cases} \tag{2}$$

where $|y_i| \leq 2047$ $(1 \leq i \leq n)$.

The histogram built from each component of $\boldsymbol{y}$ shows a shape that resembles the Laplace distribution although the former is a discrete distribution while the latter is a continuous one, with a considerable less amount of dispersion than the distribution of $\boldsymbol{x}$. The right part of Fig. 4 displays the histogram of the distribution obtained after the application of the differentiation process on the ECG signal.

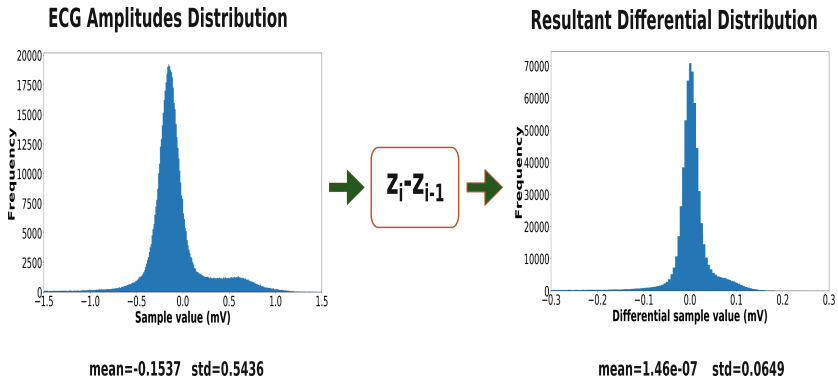

Fig. 4. Histograms for raw ECG signal distribution (left) and the resultant distribution after the differentiation process (right).

4.2 Signal Quantization

The next step in the signal processing pipeline aims to translate the information contained in the differential signals into a domain defined over a smaller alphabet set. Let's define Q as the odd number of quantization levels under which the quantization will take place. Any quantized symbol can be defined only on the set of integers $\{0, 1, \ldots, Q-1\}$. The quantization process is carried out with a simple ranking system that assigns each sample its corresponding quantized symbol depending on its differential amplitude value.

Hereafter, let us denote a sequence of quantized symbols of length n by a string $\boldsymbol{x}^n$ over Σ_Q where $m = Q$. The ith quantized symbol x_i on the sequence $\boldsymbol{x}^n = x_1 x_2 \ldots x_n \in \Sigma_Q^n$ can be obtained from the differential sequence $\boldsymbol{y}^n$ and the set of quantization parameters $\{q_0, q_1, \ldots, q_{Q-2}\}$ where q_l's $(0 \leq l \leq Q-2)$ are reals and $q_i < q_j \quad (0 \leq i < j \leq Q-2)$.

Then, the quantization rule is given as follows:

$$x_i = \begin{cases} 0 & y_i \leq q_0, \\ l & q_{l-1} < y_i \leq q_l \\ Q-2 & y_i > q_{Q-2}. \end{cases} \tag{3}$$

The quantization procedure is illustrated on Fig. 5. Previous experiments with different quantization levels have shown that the algorithm perform at its best when $Q = 7$. Next, for the definition of the quantization parameters, lets consider the *percentile* P_r as the value on the ECG distribution below which a percentage $r(\%)$ of the samples is allocated. Then, the quantization parameters are given as:

$$q_0 = P_{1.5}, \quad q_1 = P_{10}, \quad q_2 = P_{25}, \quad q_3 = P_{75}, \quad q_4 = P_{90}, \quad q_5 = P_{98.5} \tag{4}$$

An example of the quantization operation over a differential distribution is presented on Fig. 5 for a value of $Q = 7$.

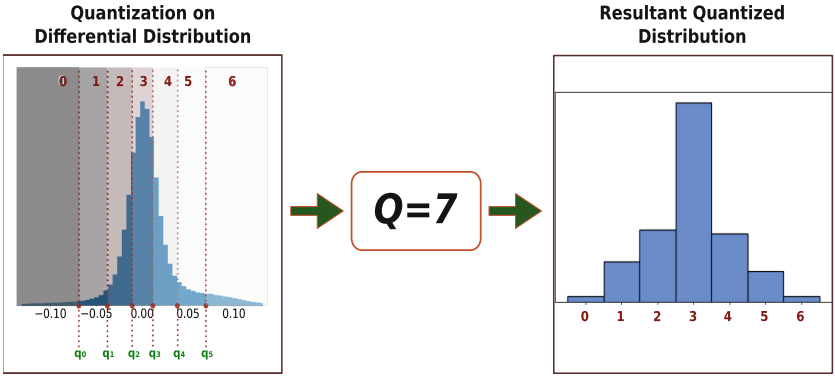

Fig. 5. Quantization operation on a differential ECG distribution (left) and the resultant quantized distribution (right). The location of the quantization parameters and the corresponding interval for each symbol are highlighted.

4.3 Training Data and Antidictinary AD Generation

The antidictionary set $\mathcal{A}$ to be used in the encoding process is generated from a segment of ECG data in a preprocessing stage as follows:

Step 1. First, let k be a certain positive integer denoting the total number of training files from which the antidictionary $\mathcal{A}$ will be constructed. Each training file $\boldsymbol{u}_i$ $(1 \leq i \leq k)$ consists of 5 ECG waveforms (roughly between 3 and 5.5 seconds of ECG recording). Here, a waveform is defined as the portion of the signal covered by one R-R interval, as is described on the left waveform on Fig. 1. For each training file $\boldsymbol{u}_i$ an antidictionary set $\mathcal{A}(\boldsymbol{u}_i)$ is constructed and the process results in the family of antidictionaries

$$\mathcal{A}_K = \{\mathcal{A}(\boldsymbol{u}_1), \mathcal{A}(\boldsymbol{u}_2), \ldots, \mathcal{A}(\boldsymbol{u}_k)\}\,.$$

The process is described on Fig. 6.

Step 2. The antidictionary set $\mathcal{A}$ is conformed primarily by the set of MFWs that show a higher frequency of occurrence among all the generated antidictionaries $\mathcal{A}(\boldsymbol{u}_1), \mathcal{A}(\boldsymbol{u}_2), \ldots, \mathcal{A}(\boldsymbol{u}_k)$ in $\mathcal{A}_k$. Due to the periodic nature of the ECG signal, some MFWs are expected to appear constantly among the majority of the generated antidictionaries. However, the dynamic variations in the amplitude and periods of the training waveforms induce some variability on the frequency of occurrence of some MFWs. Given an MFW $\boldsymbol{w}$, the frequency of occurrence $f(\boldsymbol{w})$ on $\boldsymbol{w}$ is given by

$$f(\boldsymbol{w}) = |\{i \,|\, \boldsymbol{w} \in \mathcal{A}(\boldsymbol{u}_i), 1 \leq i \leq k\}|\,. \tag{5}$$

Step 3. Based on those f values, the MFWs are sorted and finally, the antidictionary set $\mathcal{A}$ can then be built with the MFWs that exhibit a relatively high frequency of occurrence. Experimental trials show that the MFWs with the higher frequency of occurrence are in general strings of length one or two. Those short strings usually perform poorly when implemented in the FSM model in

the detection scheme. In that sense, for the construction of $\mathcal{A}$ the constraint of choosing MFWs of length greater than or equal to 3 is imposed in order to achieve better performance in the detection algorithm.

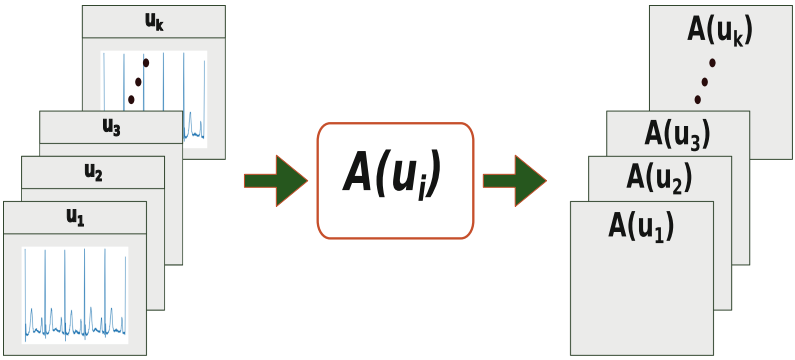

Fig. 6. Antidictionary set construction from the ECG training files set.

4.4 FSM Construction and Detection Criteria

With the appropriate set of MFWs picked from the antidictionary set $\mathcal{A}$, the FSM can be build alongside the accompanying probability model. Given a set of MFWs defined over an alphabet Σ_Q, in the implementation of the FSM each state is modeled with two memory registers for each outgoing edge associated with symbol $c \in \Sigma_Q$. The first register acts as a pointer to the next state reached through symbol c and the second register is implemented as a counter that holds the number of transitions to the next state though c. For the particular case of the FSM with $Q = 3$ on Fig. 2, there are seven states in total with three outgoing edges per state. Thus, the number of memory registers necessary for the implementation of the FSM would be equal to 42.

Once the FSM model is constructed, the transition probabilities are calculated by performing a second pass in the training data and updating the corresponding counter for each state transition.

Let $\boldsymbol{x}^n = x_1 x_2 \dots x_n$ be a string being processed with the detection algorithm by means of a FSM constructed with the appropriate probabilistic model. For $1 \leq i \leq n$ and a given number $d > 0$, the *instantaneous* compression ratio R_i defined on a sliding window w_i of size d is given by

$$R_i = \begin{cases} \dfrac{1}{d} \displaystyle\sum_{k=i-d+2}^{i+1} \ln \frac{1}{P(x_k|s_{k-1})} & i - d > 0, \\ \dfrac{1}{i} \displaystyle\sum_{k=2}^{i+1} \ln \frac{1}{P(x_k|s_{k-1})} & i - d \leq 0. \end{cases} \tag{6}$$

where $P(x_k|s_{k-1})$ is the transition probability defined in (1).

A threshold value T is chosen such as an instantaneous compression ratio R_i greater than T will signal the presence of an arrhythmia pattern in the input string. Figure 7 illustrates the case of a positive detection when the PCV located around 156 s time stamp causes an increase on the compression ratio, effectively surpassing the set threshold (2.5).

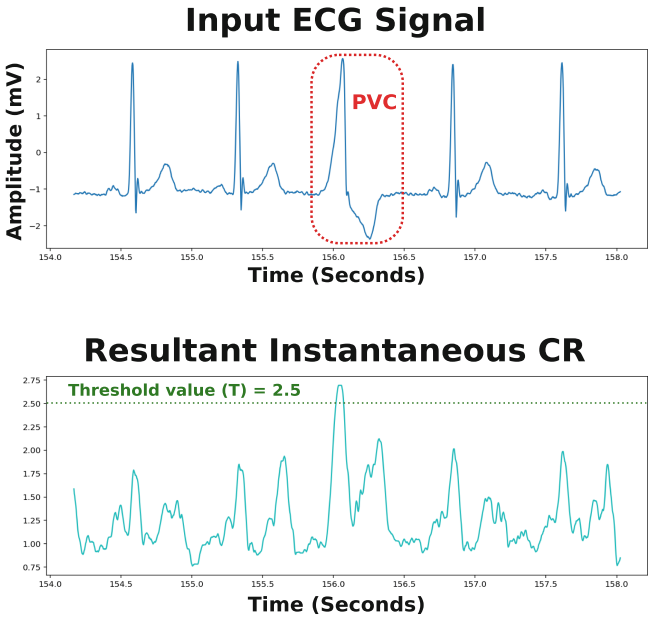

Fig. 7. Positive detection of a PVC heartbeat. The top figure displays an ECG sequence containing one PVC heartbeat while the bottom figure shows how the Instantaneous Compression Ratio goes above the set threshold value (T = 2.5), likely due to a forbidden pattern occurring within PVC.

5 Offline Preprocessing, Model Selection and Accuracy Assessment of FSM Models

In this section we describe the process involving the experimentation with the ECG records to obtain the best performance FSM models in an offline fashion. The test signals used for the experiments were taken from the MIT-BIH Arrhythmia Database, a library of ECG records commonly used for the evaluation of ECG arrhythmia detectors. It consists of 48 records, each one comprising 30 min of ECG recording on two channels digitized at 360 samples per second per channel at an 11-bit resolution spanning a 10 mV dynamic range. Each ECG record contains annotations given by two or more cardiologists, thus providing a medical grade benchmark for the assessment of the quality of arrhythmia detectors [11,12].

In each experiment, training sets consisting of 50 training files (one training file containing 5 ECG waveforms, and one waveform consisting of the portion of ECG data covering the R-R segment) were used for the constructions of the antidictionaries. Only portions of the ECG signals from the MIT-BIH Arrhythmia Database annotated as "Normal" were employed for the construction of the training sets.

The MFWs from the antidictionary set where then sorted according to their f values, as described on Sect. 4.3. A common antidictionary set was then constructed from the top 20 MFWs on the sorted set. From the common antidictionary set, 190 different FSM models where then constructed taking into consideration all possible combinations of 2 MFWs.

The transition probabilities for each FSM model were calculated from the segment of training data previously used for the construction of the antidictionaries and then each FSM was tested with the whole ECG sequence. The accompanying annotations files from the MIT-BIH Arrhythmia Database where used for the posterior calculation of the detection evaluation metrics sensitivity and specificity. The sensitivity, or true positive rate, measures the ratio of true arrhythmia heartbeats detected while the specificity measures the ratio of normal heartbeats identified as such by the algorithm.

Table 1 shows the results obtained after processing 6 records from the database. The differentiation process resulted on distributions centered around zero with shapes similar to the distribution shown on the right part of Fig. 4. For the determination of the set of quantization parameters, the percentiles values where calculated from the distribution of ECG samples obtained within the first minute of recording (corresponding to 21,600 samples for records from the MIT-BIH Arrhythmia Database).

The results on Table 1 for records 105, 205 and 228 correspond to cases with FSM models of 2 MFWs, while in the cases of records 201, 215 and 221 slightly bigger models of 4 MFWs were employed to improve detection accuracy.

Table 2 contains the average metrics (sensitivity and specificity) obtained after processing the 6 aforementioned ECG records, where the metrics of other methods available on literature are given for comparison purposes.

While the proposed detection algorithm achieves high average values of Sensitivity, the average Specificity suffers in comparison with other methods, as described on Table 2. It is important to notice, however, that no prior treatment of the test signals was carried for conditioning or noise removal. It is very plausible that improvements on Specificity would follow with the use of appropriate methods for noise removal.

For the detection process, a sliding window size of $d = 25$ symbols was used for the calculation of the instantaneous compression ratio R_i and a dynamic range of threshold values T (in the range 1.8 to 3.2) was used to have an insight on how the variability on T can affect the detection process.

Table 3 shows a comparative description of the antidictionaries and FSM implementation characteristics for the proposed detection system and the detection system proposed in [3]. For the calculation of the antidictionary size values

presented on Table 2, a byte has been assigned to describe every quantized symbol that conform an MFW.

Figure 8 displays the Receiver Operating Characteristics (ROC) curves for three different FSM built for record 228, evaluated on a range of threshold values T raging from 1.8 to 3.2 on increments of 0.01 units. The set of MFWs for FSM Model-1 is $AD_1 = \{656, 513\}$ while the antidictionary sets for the remaining two models (FSM Model-2 and FSM Model-3) are $AD_2 = \{656, 5351\}$ and $AD_2 = \{013, 514\}$, respectively.

A common MFW, 656, can be found on the antidictionary set of the two best performing FSM models (FSM Model-1 and FSM Model-2), thus suggesting that MFW very likely corresponds to a forbidden pattern within the PVCs morphology.

Table 1. Table of results (%) for the detection of PVC on 6 ECG records from the MIT-BIH database.

Record	Sen.	Spec.
105	100	94.77
201	98.98	98.40
205	97.18	99.57
215	93.29	79.74
221	97.97	94.43
228	97.79	96.44
Average	**97.53**	**93.89**

6 Implementation on a Mobile Platform

The second stage of experimentation consisted on the port of the detection algorithm into a mobile environment for the evaluation of performance at online operation. The experimental setup is described on Fig. 9. A pre-trained FSM model has been ported in addition to a quantization stage for the processing of a stream of ECG samples on real time. Continuing with the same methodology used on off-line experimentation, the records from the MIT-BIH Arrhythmia databased have been employed for testing the algorithm.

6.1 Wearable ECG Hardware Characteristics

A custom hardware configuration has been used to emulate the characteristics of a wearable ECG sensor handling the wireless transmissions of the ECG samples obtained from the annotated files on the MIT-BIH Arrhythmia database. The virtual wearable monitor is based around the ESP32-WROOM-32 Microcontroller Unint from Espressif Systems [16]. The ESP32-WROOM-32 contains the

Table 2. Comparison of the proposed method with other arrhythmia detectors.

Algorithm	Sensitivity	Specificity
Proposed method	**97.53**	**93.89**
Ota et al. [3]	97.9	98.6
Ittatinut et al. [13]	91.05	99.55
Adnane et al. [14]	97.21	98.67
Alajlan et al. [15]	100	93.71

Table 3. Antidictionaries and FSM implementation characteristics for quantized signals from six different ECG records. Results obtained previously in [3] are given for comparison purposes.

ECG record	105	201	205	215	221	228
Results obtained on Ota et al. [3]						
Number of MFWs	281	90	56	178	85	189
AD size (bits)	3,586	996	436	1,792	988	2,316
FSM size (kB)	24.2	6.5	2.6	11.5	6.5	15.4
Results obtained with the proposed method						
Number of MFWs	2	4	2	4	4	2
AD size (bits)	48	120	48	144	112	48
FSM size (kB)	**1.6**	**3.2**	**1.6**	**3.6**	**2.5**	**1.6**

ESP32 System on a Chip (SoC) device alongside flash memory and the hardware requirements to achieving low power Wi-Fi and Bluetooth Low Energy (LE) communication.

The Bluetooth LE standard enables low power communication between the ECG sensor and the mobile device and at the same time facilitates the easy implementation of the services both in the client and the server side, reducing the development time of the mobile application.

The ECG samples have been read from binary files stored on a SD card with the use of one of the multiple on-board Serial Peripheral Interface (SPI) buses available on the ESP32-WROOM-32 device. The ESP32 (SoC) device supports a broad range of open software initiatives, like the Arduino Open Software project. In our case, the whole configuration of the ESP32 core device was carried out on top of the SPI and Bluetooth libraries freely provided by Espressif Systems and the open source community [17].

In accordance to the Bluetooth LE specification, a custom Bluetooth Service and its corresponding Characteristic were implemented both in the wearable device and the mobile application [18]. Two randomly generated Universally Unique IDs (UUID) where used to identify both the Service and its Characteristic. ECG samples are treated as 16 bits unsigned numbers, and two samples are transmitted every 6 mS, for a rate of 333 ECG samples per second. The Blue-

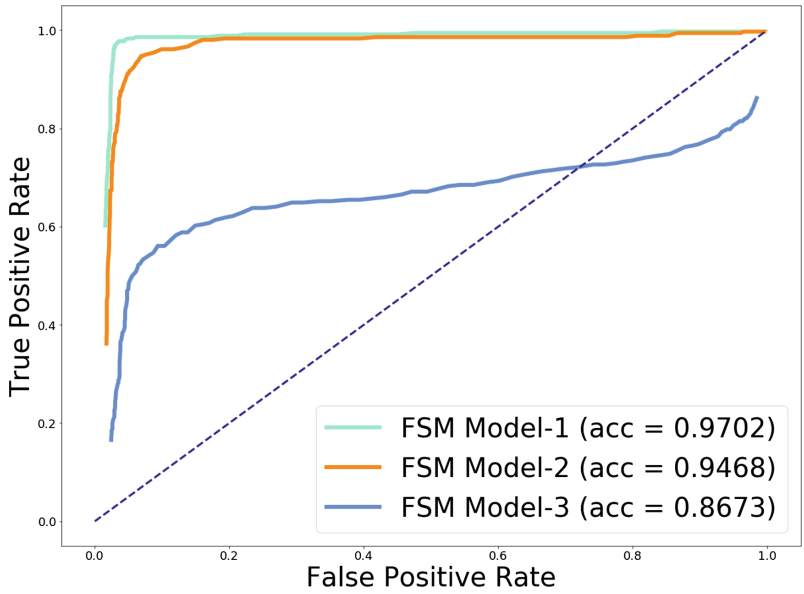

Fig. 8. Receiver Operating Characteristics curves for three different FSM trained to process record 228 under a wide range of threshold values (T). Maximum accuracy values and the corresponding threshold values for each model are given as follows: FSM Model-1 achieving 97.02% accuracy at $T = 2.56$, FSM Model-2 reaching 94.68 % at $T = 2.67$ and FSM Model-3 with 86.73% accuracy at $T = 2.63$.

tooth Characteristic is granted with the "Notify" property, and each time two samples are ready for transmission the notification alerts the mobile applications Bluetooth instance.

6.2 Mobile Application Deployment

The mobile application has been developed on the IOS mobile operating system. An object oriented approach has been adopted for the implementation of the quantization and FSM related data structures, to speed up development and facilitate code readability.

The deployed application was evaluated with Apple's Xcode development environment and tested on an Iphone 6s device. By using Xcode's memory profiler and benchmark tools, the performance of the application was evaluated with an average of 30MB of memory and 65% of CPU usage on one of the cores of the mobile device while processing the ECG samples in an on-line fashion. Figure 10 shows a screenshot of the running mobile application alongside the prototype of the ECG sensor. An USB connection is used to upload the firmware on the ESP32-WROOM-32 unit and to power it during operation.

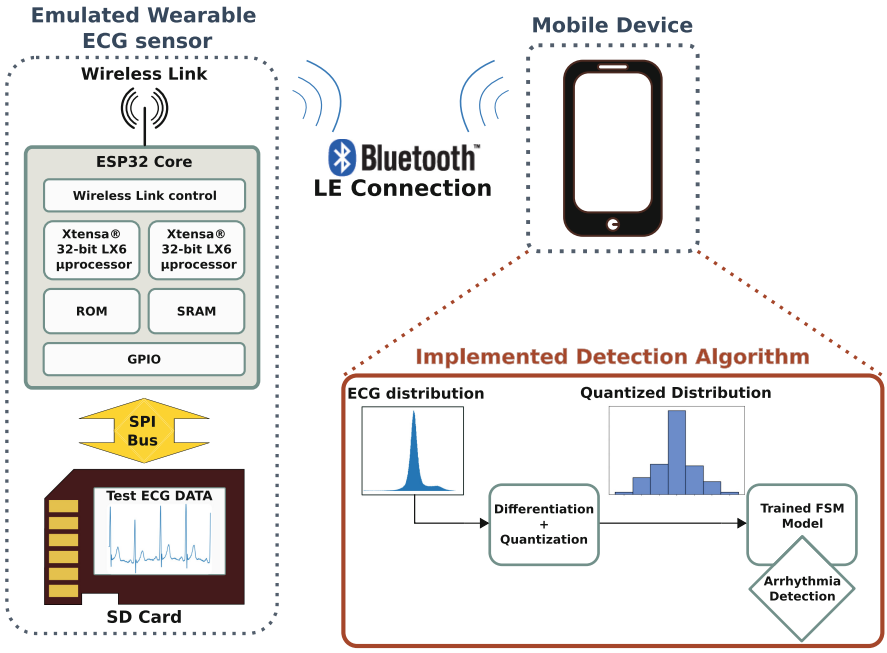

Fig. 9. Schematic digram of the experimental setup used for the evaluation of the detection algorithm on an mobile platform.

7 Discussion

In order to increase the sensitivity values on the measurements, further care should be taken for handling baseline wandering, mains interference and other sources of noise.

The offline processing of the records for the determination of the best set of antidictionaries and the construction of FSM models can prove to be a computationally intensive process, as each FSM model is evaluated with the entire ECG sequence over a range of threshold values. Next stages in our research efforts include the identification of specific MFWs patterns for PVCs and other types of arrhythmias to narrow down the pool of target MFWs and simplify the preprocessing stage.

The mobile application performed with a constant average usage of 30 MB of system memory while running a FSM of 9 nodes in the background and processing the ECG record 201 from the MIT-BIH database. The use of bigger FSM models for increasing accuracy should not lead to excessive increase on memory usage.

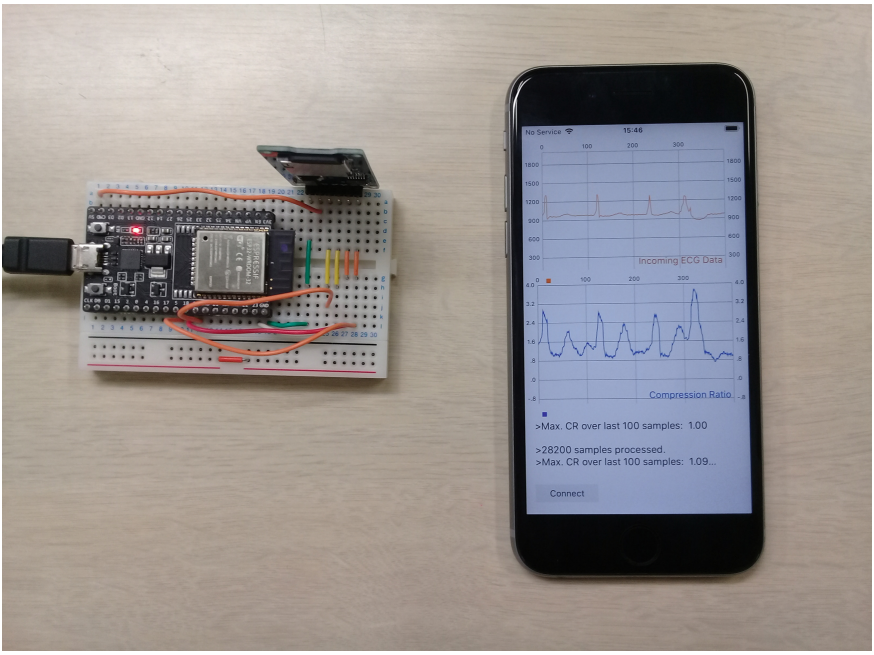

Fig. 10. The experimental setup for the online evaluation of the trained FSM models. The emulated ECG sensor (on the left) transmits the ECG samples through Bluetooth LE while in the mobile application the quantization and posterior processing in the FSM is effectuated to produce the output CR waveform displayed on the phone screen.

8 Conclusion

A system for the discrimination of irregular ECG patterns based on the scheme of antidictionary encoding applied to quantized signals has been presented, with a proof of concept port of a pre-trained FSM model into a mobile application.

The rescaling of the ECG distribution with the differentiation and quantization operations results on lower space complexity requirements for the implementation of the FSM probabilistic models. This is evidenced on Table 3, where an average size of 2.35 KB is calculated for the models constructed with the proposed approach while the models designed from binary ECG sequences require an average of 11.11 kB. This is further evidenced with the relatively low memory resources usage (30.5 MB) for online processing of ECG samples on the mobile application.

The achieved average metrics of sensitivity (97.53%) renders the proposed detection algorithm as a feasible alternative for PVC detection. Higher sensitivity values can be achieved with approaches such as the Gaussian Process Classifier (GPC) method suggested in [15], this at the expense of using bigger segments of training data and using a mix of time and frequency domain features to differentiate the pathological heartbeats.

Further research efforts aiming to increase the average specificity metrics could include the evaluation of additional time domain features, such as the R-R interval assessment made in [13] and band-limiting the ECG signal in a narrow frequency band to eliminate high frequency noise, as happens with the Discrete Wavelet Transform (DWT) method used on [14].

Besides, a deep dive in more specific details about the characteristic forbidden patterns that appear in each type of heartbeat could lead to the extension of the algorithm to a multi-class classification category.

References

1. Dias, D., Paulo Silva Cunha, J.: Wearable health devices—vital sign monitoring, systems and technologies. Sensors **18**(8), 2414 (2018)
2. Crochemore, M., Mignosi, F., Restivo, A., Salemi, S.: Text compression using antidictionaries. In: Wiedermann, J., van Emde Boas, P., Nielsen, M. (eds.) ICALP 1999. LNCS, vol. 1644, pp. 261–270. Springer, Heidelberg (1999). https://doi.org/10.1007/3-540-48523-6_23. https://hal-upec-upem.archives-ouvertes.fr/hal-00619991/document
3. Ota, T., Morita, H., de Lind van Wijngaarden, A.J.: Real-time and memory-efficient arrhythmia detection in ECG monitors using antidictionary coding. IEICE Fundam. **E96–A**(12), 2343–2350 (2013)
4. Frias, G., Morita, H., Ota, T.: Anomaly detection on quantized ECG signals by the use of antidictionary coding. In: Proceedings of the 41st Symposium on Information Theory and its Applications, December 2018
5. Rajni, R., Kaur, I.: Electrocardiogram signal analysis - an overview. Int. J. Comput. Appl. **84**(7), 22–25 (2013)
6. Mayo Clinic: Premature ventricular contractions (PVCs), February 2018. https://www.mayoclinic.org/diseases-conditions/premature-ventricular-contractions/symptoms-causes/syc-20376757
7. ECGwaves.com: Premature Ventricular Contractions (premature ventricular complex, premature ventricular beats): ECG and clinical implications (2018). https://ecgwaves.com/premature-ventricular-contractions-complex-beats-ecg/
8. Ota, T., Morita, H.: On-line electrocardiogram lossless compression using antidictionary codes for a finite alphabet. IEICE Trans. Inf. Syst. **E93–D**(12), 3384–3391 (2010)
9. Zhao, Z., Zhang, Y.: SQI quality evaluation mechanism of single-lead ECG signal based on simple heuristic fusion and fuzzy comprehensive evaluation. Front. Physiol. **9**, 727 (2018)
10. Tziakouri, M., et al.: Classification of AF and other arrhythmias froma short segment of ECG using dynamic time warping. In: Computing in Cardiology, vol. 44, pp. 1–4 (2017)
11. Moody, G.B., Mark, R.G.: The impact of the MIT-BIH arrhythmia database. IEEE Eng. Med. Biol. Mag. **20**, 45–50 (2001)
12. Goldberger, A.L., Amaral, L., et al.: PhysioBank, PhysioToolkit, and PhysioNet: components of a new research resource for complex physiologic signals. AHA - Circulation **101**(23), E215–20 (2000)
13. Ittatirut, S., Lek-uthai, A., Teeramongkonrasmee, A.: Detection of premature ventricular contraction for real-time applications. In: 2013 10th International Conference on Electrical Engineering/Electronics, Computer, Telecommunications and

Information Technology, pp. 1–5, May 2013. https://doi.org/10.1109/ECTICon.2013.6559531
14. Adnane, M., Belouchrani, A.: Premature ventricular contraction arrhythmia detection using wavelet coefficients. In: 2013 8th International Workshop on Systems, Signal Processing and their Applications (WoSSPA), pp. 170–173, May 2013. https://doi.org/10.1109/WoSSPA.2013.6602356
15. Alajlan, N., Bazi, Y., Melgani, F., Malek, S., Bencherif, M.A.: Detection of premature ventricular contraction arrhythmias in electrocardiogram signals with kernel methods. Sig. Image Video Process. **8**(5), 931–942 (2014). https://doi.org/10.1007/s11760-012-0339-8
16. Espressif Systems: Esp32-wroom-32 datasheet. https://www.espressif.com/sites/default/files/documentation/esp32-wroom-32_datasheet_en.pdf
17. Espressif Systems: Repository: Arduino core for esp32 wifi chip. https://github.com/espressif/arduino-esp32
18. The Bluetooth Special Interest Group (Bluetooth SIG): GATT services. https://www.bluetooth.com/specifications/gatt/services